Volume and composition dependence of direct and indirect band gaps in ordered ternary III-V semiconductor compounds: A screened-exchange LDA study

S. Picozzi and A. Continenza
Istituto Nazionale di Fisica della Materia (INFM), Dipartimento di Fisica, Università degli Studi di L'Aquila, 67010 Coppito (L'Aquila), Italy

R. Asahi,* W. Mannstadt, and A. J. Freeman
Department of Physics and Astronomy and Materials Research Center, Northwestern University, Evanston, Illinois 60208

W. Wolf and E. Wimmer
Molecular Simulations Inc., Orsay, France

C. B. Geller
Bettis Atomic Power Laboratory, West Mifflin, Pennsylvania
(Received 27 September 1999)

Quasiparticle electronic band structures for ternary InGaAs and InGaSb systems, modeled by a luzonite structure, have been obtained using the screened-exchange local-density approximation approach. We focus our attention on energy transitions relevant for the electron-hole pair lifetime and, in particular, on the direct ($E^{\bar{\Gamma}-\bar{\Gamma}}$) and lowest indirect ($E^{\bar{\Gamma}-\bar{L}}$) band gaps as a function of volume, common anionic species, and composition. All these degrees of freedom can be used to tune the transitions considered: as a first result, a large range of band gaps (almost 1 eV) can be obtained by varying the lattice constants within a few percent with respect to their equilibrium values. Moreover, the lowest indirect transition can be strongly reduced by replacing As with Sb. Finally, the composition dependence of these transitions shows that, due to symmetry properties of the potential in ternary luzonites, In-rich systems have the smallest indirect band gaps of all compounds investigated in this work.

I. INTRODUCTION

Ternary and quaternary[1] III-V semiconductor alloys have been the subject of many experimental[2] and theoretical[3] studies, due to their numerous potential technological applications such as high-speed electronic circuits and optoelectronic devices. In particular, the efficiency of thermophotovoltaic devices depends strongly on carrier diffusion lengths, which is related to the carrier effective mass and electron-hole pair lifetime. Both the effective mass and carrier lifetime are greatly affected by details of the band structure. Realistic descriptions of alloys need to take into account the balance between random distributions [see the special quasirandom (SQS) approach proposed by Wei *et al.*[4]] and effects such as short-range ordering,[5] phase segregation, and spontaneous CuPt ordering.[6] For instance, it is unclear whether *like* atoms (i.e., Ga-Ga in InGaAs systems) tend to associate (''clustering'') (Ref. 7) or *unlike* atoms (i.e., In-Ga in InGaAs systems) aggregate (''anticlustering'').[8]

With an aim at meeting specific technological requirements, the present work focuses on understanding key chemical and structural effects which influence critical points in the conduction band of III-V alloys. In particular, we studied ordered $In_xGa_{1-x}X$ systems (with $x=\frac{1}{4},\frac{3}{4}$ and the anion X being As or Sb), which are promising materials for thermo–photovoltaic (TPV) devices. Moreover, we focus on the luzonite structure and in particular on the $\bar{\Gamma}-\bar{\Gamma}$ and $\bar{\Gamma}-\bar{L}$ transitions (here and in the following we denote the electronic states of ternary compounds with an overbar), which can play a key role in determining the carrier lifetime in these materials. Although the structure of the alloys used in TPV devices is certainly more complex, there are several good reasons to focus on ordered luzonite structures. First, these systems show perfect anticlustering (since the first cationic shell around a given cation—i.e., Ga—consists of all cations of a different atomic species—i.e., In) which, according to previous total-energy calculations,[9] is indicated to be energetically favored. In addition, previous *ab initio* calculations[10] performed by Wei and Zunger on III-V semiconductor alloys (such as $GaAs_xSb_{1-x}$ and $Al_xGa_{1-x}As$) taking into account structural disorder have demonstrated that ordered luzonite structures show direct band gaps similar to disordered alloys (see Fig. 13 of Ref. 10) in good agreement with experimental data. Finally, luzonite has a cubic structure and is therefore very suitable for studying the effects of an isotropic compression or expansion on the $\bar{\Gamma}-\bar{\Gamma}$ and $\bar{\Gamma}-\bar{L}$ transitions in which we are interested.

It is well known that for III-V compounds of interest for TPV applications, the widely used density-functional theory (DFT) in the local-density approximation (LDA) (Ref. 11) gives unphysical negative band gaps and incorrect excitation energies. Therefore we use the LDA wave functions from accurate full-potential linearized augmented plane-wave (FLAPW)[12] calculations as a basis for a screened-exchange LDA (SX-LDA) approach[13] for obtaining quasiparticle energies. This scheme, recently proposed within the pseudopotential framework[13,14] and implemented in the FLAPW method,[15,16] goes beyond DFT by modelling the exchange

hole within a nonlocal scheme. Previous calculations[16] have shown that self-consistent SX-LDA gives excellent band gaps for $s-p$ bonding binary semiconductors as well as accurate electronic band structures for both occupied and unoccupied states, so that we expect reliable values for the $\overline{\Gamma}-\overline{\Gamma}$ and $\overline{\Gamma}-\overline{L}$ transitions. We recall that in III-V semiconductors carriers in conduction side band valleys like those at L and X have much higher effective masses than those in the primary valley at Γ, because the band curvature at Γ is steeper.[17] It follows that valence-band electrons that are excited into the conduction side band valleys at L or X will have relatively short diffusion lengths and thus will have a relatively low probability of being collected at the leads of a TPV device. Carriers can be scattered from Γ into the side valleys by random thermal excitations (i.e., phonons) and by the atomic disorder existing especially in ternary and quaternary alloys. Therefore if the L local minima in the conduction band are sufficiently close in energy to the Γ point a significant amount of useful light could be consumed in indirect transitions from the valence-band maximum to the secondary minima. As discussed, such indirect optical transitions would contribute little to the output power of the device, since the diffusion lengths of such heavy electrons would be short. Moreover, carriers originally in the conduction-band minimum at Γ also may be scattered into the L or X side valleys by nonradiative processes such as Auger or scattering due to impurities and alloy disorder. In essence, then, these indirect transitions are a loss mechanism competing with the direct $\Gamma-\Gamma$ transition. As a consequence, in addition to the $\overline{\Gamma}-\overline{\Gamma}(E^{\overline{\Gamma}-\overline{\Gamma}})$ and $\overline{\Gamma}-\overline{L}$ gaps ($E^{\overline{\Gamma}-\overline{L}}$), it is particularly important to examine the so-called ''$\overline{\Gamma}-\overline{L}$ separation,'' $\Delta E^{\overline{\Gamma}-\overline{L}}=E^{\overline{\Gamma}-\overline{L}}-E^{\overline{\Gamma}-\overline{\Gamma}}$. Moreover, we stress that in a perfectly ordered material, electronic transitions from $\overline{\Gamma}$ to $\overline{L}$ need to be assisted by phonons, whereas in disordered alloys, the selection rules are softened by effective backfolding of states to $\overline{\Gamma}$; this effect may enhance the probability of transitions into the $\overline{L}$ valley.

This work is organized as follows: in Sec. II the computational and structural parameters used in the calculations are illustrated; in Sec. III we discuss the SX-LDA electronic properties, focusing on the band structures for binary and ternary compounds obtained within SX-LDA and, in particular, on the trends in direct and indirect band gaps as a function of pressure and composition; Sec. IV summarizes our results and draws some conclusions.

II. STRUCTURAL AND COMPUTATIONAL DETAILS

Accurate FLAPW functions were generated within the DFT-LDA framework, using an exchange-correlation potential with the Hedin-Lundqvist parametrization.[18] We considered a plane-wave basis set with a cutoff $k_{max}=3.0$ a.u. and an expansion in spherical harmonics with $l_{max}=8$ inside the muffin-tin spheres, with muffin-tin radii $R_{MT}^{Ga}=R_{MT}^{As}=2.25$ a.u., $R_{MT}^{In}=2.50$ a.u., $R_{MT}^{Sb}=2.62$ a.u. The Brillouin zone (BZ) was sampled via the Monkhorst-Pack scheme,[19] using four special k points in the irreducible wedge. In the SX-LDA calculations, only the s and p electrons were considered as valence. The cation d states are treated as relaxed core states. For the compounds of interest here, the treatment of d states is not as crucial as in other binary semiconductors (such as GaN, ZnS, ZnSe, etc., where the cation d electrons strongly interact with the anion s state). Hence the approximation of considering only s and p states in the valence are known to give reasonable results.[20] In order to achieve convergence for the SX-LDA eigenvalues, we used 28 states (including 12 empty states). The charge density and wave functions were obtained self-consistently within the SX-LDA approach, whereas the spin-orbit coupling was treated perturbatively on the self-consistent charge density.[21]

TABLE I. Experimental lattice constants (values in Å from Ref. 22) for the zinc-blende binary constituents and cubic lattice constants for luzonite structures at different concentrations, according to Vegard's rule.

InAs	GaAs	$In_{0.25}Ga_{0.75}As$	$In_{0.75}Ga_{0.25}As$
6.058	5.653	5.755	5.957
InSb	GaSb	$In_{0.25}Ga_{0.75}Sb$	$In_{0.75}Ga_{0.25}Sb$
6.479	6.096	6.192	6.383

We used experimental 300 K lattice constants[22] (the FLAPW calculated values are within 0.5% of experiment[20]) for the zinc-blende binary compounds (shown in Table I) and the equilibrium lattice constants for the ternaries, $A_xB_{1-x}C$, were chosen according to Vegard's rule:[23] $a_{Vegard}=(x)a_{AC}+(1-x)a_{BC}$ (see Table I). The unit cell for the luzonite structure[24] contains eight atoms, whose internal positions have been fully relaxed according to the *ab initio* atomic forces.

III. SX-LDA ELECTRONIC PROPERTIES

A. Band structure

We first discuss the SX-LDA results obtained for direct and indirect band gaps in the pure binary compounds. The LDA, SX-LDA, and experimental values[17,25] at selected important symmetry points are compared in Table II. First, it is evident that the difference between the SX-LDA and bare LDA values is k dependent, so that the corrections due to the SX-LDA approach go well beyond a rigid shift to higher energies (i.e., the so-called ''scissor'' operator). Moreover, the overall agreement with experimental data is quite good. We note that the SX-LDA method seems to work very well for the In compounds, whereas it is not as accurate in recovering the discrepancy between pure LDA values and experiment for Ga compounds. Therefore we expect that the values obtained for ternary In-rich compounds are very close to experiment, whereas a larger error could affect predictions for the Ga-rich systems. In addition, we recall that the SX-LDA results could be corrected further using a *semiempirical* procedure,[26] based on experimental data for binaries and LDA values for the ternaries (see Ref. 27 for details). However, we stress that absolute values for direct and indirect band gaps are not the focus of the present work, which is rather to determine the different *trends* of the transitions considered as a function of structure and composition. Also, we should remark that we are not aware of any experimental

TABLE II. LDA, SX-LDA, and experimental values (in eV) of direct and indirect band gaps for the binary constituents (spin-orbit coupling included). The valence-band maximum is taken as the zero of the energy scale.

		$\Gamma-\Gamma$	$\Gamma-L$	$\Gamma-X$
	LDA	−0.53	0.69	1.31
InAs	SX-LDA	0.44	1.63	2.14
	expt	0.42[a]	1.66[b]	2.16[b]
	LDA	−0.57	0.19	0.99
InSb	SX-LDA	0.30	0.90	1.59
	expt	0.24[c]		1.79[c]
	LDA	0.25	0.79	1.27
GaAs	SX-LDA	1.20	1.66	2.06
	expt	1.52[c]	1.81[c]	1.98[c]
	LDA	−0.3	0.07	0.58
GaSb	SX-LDA	0.51	0.71	1.14
	expt	0.81[d]	1.09[d]	

[a]Ref. 17.
[b]Ref. 25.
[c]See Ref. 16 and references therein.
[d]Ref. 22.

data regarding the direct and indirect transitions in luzonite InGaAs and InGaSb structures. Therefore in this work we will not use any empirical correction and we will limit the discussion to SX-LDA trends as a function of different degrees of freedom.

Let us now consider the SX-LDA band structure (spin-orbit coupling excluded) of the $In_{0.75}Ga_{0.25}Sb$ luzonite system [shown in Fig. 1(b)] as compared to that of the binary constituents along the main symmetry lines [Figs. 1(a) and (c) for GaSb and InSb, respectively, within LDA (dashed line) and with SX-LDA (solid line)]. We recall that, due to folding operations[10,28] in ternary structures, the Δ line, joining Γ to X in the zinc-blende BZ, is folded onto itself so that the X point is folded back onto the center $\bar{\Gamma}$ of the ternary BZ. As shown in Ref. 10, band folding in superstructures can cause a repulsion due to the coupling of two binary states of different symmetries folded onto a state of the same symmetry in the ternary system. It is therefore interesting to compare the critical point energies calculated for the luzonite structure with the composition weighted average levels: for example, for the direct band gap in $Ga_xIn_{1-x}Sb$, the composition weighted average would be: $\langle E^{\bar{\Gamma}-\bar{\Gamma}}_{Ga_xIn_{1-x}Sb}\rangle = (x)E^{\Gamma-\Gamma}_{GaSb}+(1-x)E^{\Gamma-\Gamma}_{InSb}$, where $E^{\bar{\Gamma}-\bar{\Gamma}}$ and $E^{\Gamma-\Gamma}$ represent the direct gap for ternaries and binaries, respectively. As expected, there is an appreciable reduction ($\Delta^{\bar{\Gamma}-\bar{\Gamma}} = \langle E^{\bar{\Gamma}-\bar{\Gamma}}_{Ga_{1/4}In_{3/4}Sb}\rangle - E^{\bar{\Gamma}-\bar{\Gamma}}_{luzonite} = -0.18$ eV) of the direct band gap in going from the average band gap to the luzonite calculated value, which has to be ascribed to the above-mentioned repulsive potential.

If we now consider the $\bar{L}$ point in In-rich Sb-based luzonites, we have two *segregating* states originating from the GaSb and InSb L_{1c} zinc-blende states. As proposed in Ref. 28, the superlattice potential induces a symmetry enforced splitting between the two original states, so that the resulting luzonite states belong to different symmetries and are localized on a different cation sublattice. In fact, we note that the lowest conduction level at $\bar{L}$ has a predominant *s* character localized on the Ga site, while the second lowest level has a predominant *s* character on the In sublattice. As a result, the repulsion between these segregating states produces a strong reduction (by about 0.5 eV) of the $\bar{\Gamma}-\bar{L}$ transition in luzonite [$E^{\bar{\Gamma}-\bar{L}}_{In_{0.75}Ga_{0.25}Sb}=0.35$ eV (Ref. 29)] with respect to the average of the corresponding $\Gamma-L$ indirect gaps in the bi-

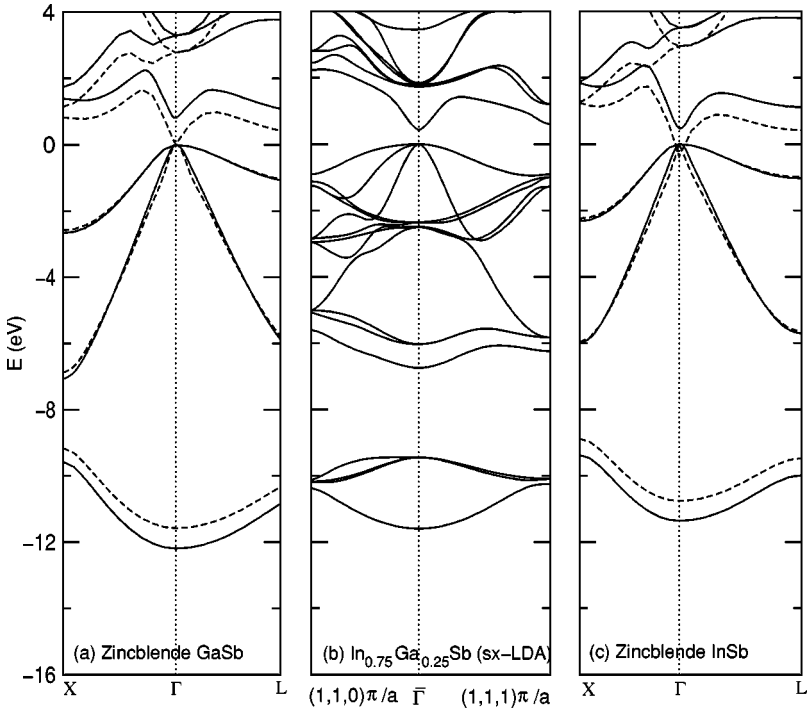

FIG. 1. Panel (a): semirelativistic LDA (dashed line) and SX-LDA (solid line) band structure for GaSb; panel (b): semirelativistic SX-LDA band structure for luzonite $In_{0.75}Ga_{0.25}Sb$; panel (c): semirelativistic LDA (dashed line) and SX-LDA (solid line) band structure for InSb.

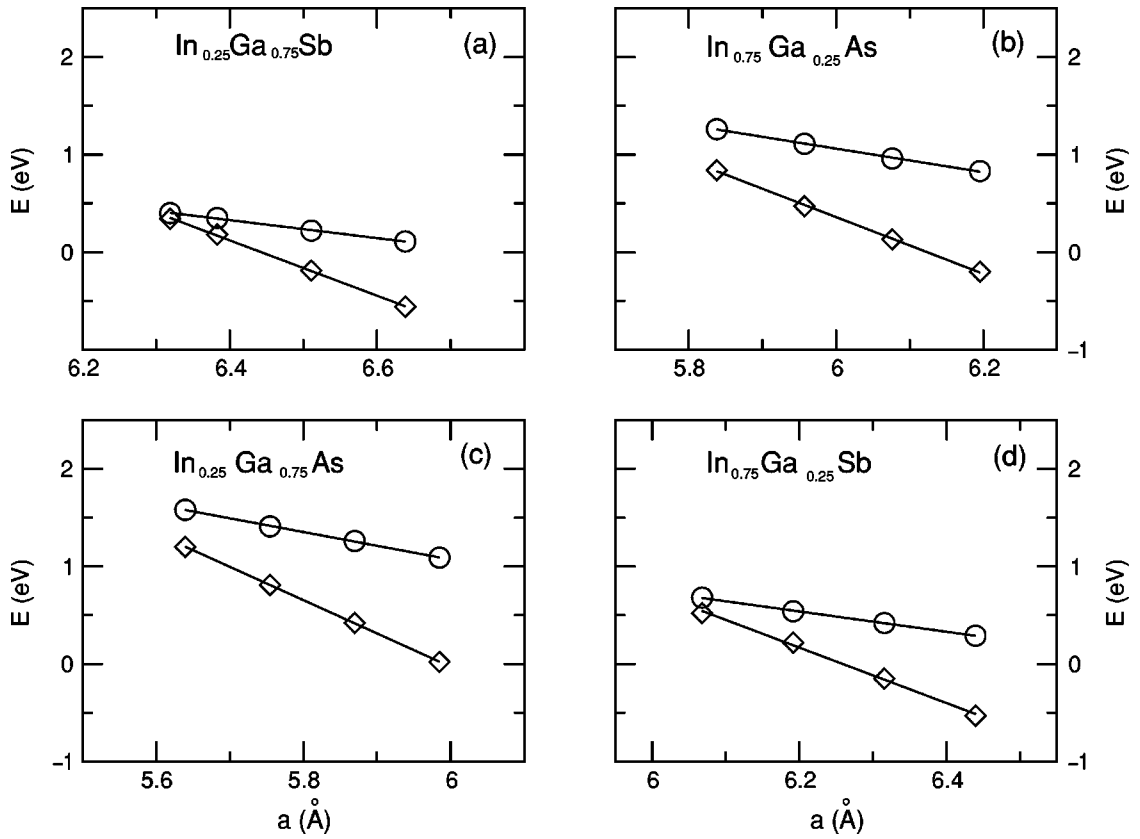

FIG. 2. SX-LDA direct (diamonds) and indirect (circles) band gaps (in eV) as a function of the cubic lattice constant (in Å) for (a) $In_{0.25}Ga_{0.75}Sb$, (b) $In_{0.75}Ga_{0.25}As$, (c) $In_{0.25}Ga_{0.75}As$, and (d) $In_{0.75}Ga_{0.25}Sb$.

nary constituents ($\langle E^{\Gamma-L}_{In_{0.75}Ga_{0.25}Sb}\rangle = 0.85$ eV). Moreover, at the $\overline{L}$ point the indirect gap reduction $\Delta^{\overline{\Gamma}-\overline{L}}$ with respect to the weighted average is even larger than at the Γ point.

B. Volume dependence of direct and indirect band gaps

In Fig. 2 we show the $\overline{\Gamma}-\overline{\Gamma}$ and $\overline{\Gamma}-\overline{L}$ transitions, obtained within self-consistent SX-LDA (spin-orbit included) as a function of the cubic lattice constant a_{latt}.[30] Panels (a) and (c) are relative to the Ga-rich Sb and As-based luzonites, respectively, whereas panels (b) and (d) are relative to In-rich As and Sb based structures, respectively. Note that the effect of volume on the direct energy gap is dramatic: in all systems considered, variations of the lattice constant of $\pm 4\%$ can change the band gap by as much as 0.7–0.8 eV. On the other hand, the effect of pressure on the $\overline{\Gamma}-\overline{L}$ transition is less evident (around 0.3 eV for changes of $\pm 4\%$ in the lattice constant), although still present.

We observe that in all structures the trend is almost perfectly linear, in agreement with deformation potential and bulk modulus measurements.[31] This fact leads to a smaller band gap as the lattice constant is increased. Most remarkably, all the compounds follow the same trend: upon expansion of the lattice, independent of the particular chemical composition, the direct and indirect energy band gaps diminish with a slope af approximately -1.6 and -0.5 eV/a.u., respectively. The value of $dE^{\Gamma-\Gamma}/da$ for $In_{0.53}Ga_{0.47}As$ (which is lattice matched to InP) determined by combining the indirectly measured band-gap pressure dependence and bulk modulus is -1.79 eV/a.u.,[31] which compares reasonably well with our calculated value, taking into account the considerable experimental uncertainty (i.e., about 0.1 eV/a.u.). It is therefore possible to tune the transition energies by varying the lattice constant. Furthermore, it is interesting to observe that our calculations predict LDA (whose values are not shown in Fig. 2) and SX-LDA approaches to give similar slopes. This is probably due to the fact that the shapes of the LDA orbitals and the SX orbitals are quite similar. Since the dependence of the gap on interatomic distances is governed mainly by changes in the overlap between orbitals, LDA and SX are expected to give the same trends. Furthermore, since it is well known that LDA can predict with good accuracy the band-gap behavior as a function of pressure, we may expect SX-LDA to also give correct results (at least for In rich compounds) both for the band-gap magnitude and its pressure dependence.

We show in Fig. 3 the $\overline{\Gamma}-\overline{L}$ separation as a function of lattice parameter for all the luzonite systems considered: as shown in the figure, the $\overline{\Gamma}-\overline{L}$ separation energy increases in all the systems with a slope of about 1 eV/a.u. In discussing Figs. 2 and 3, we note that two major effects determine energy band gaps in III-V semiconductors, namely: (i) the splitting of bonding and antibonding states (valence band and conduction band) due to chemical interactions between As (Sb) s,p states with Ga (In) s,p states and (ii) the width of each band. As cations and anions are brought into closer contact by a reduction of the lattice parameter, the splitting between bonding and antibonding states increases, which

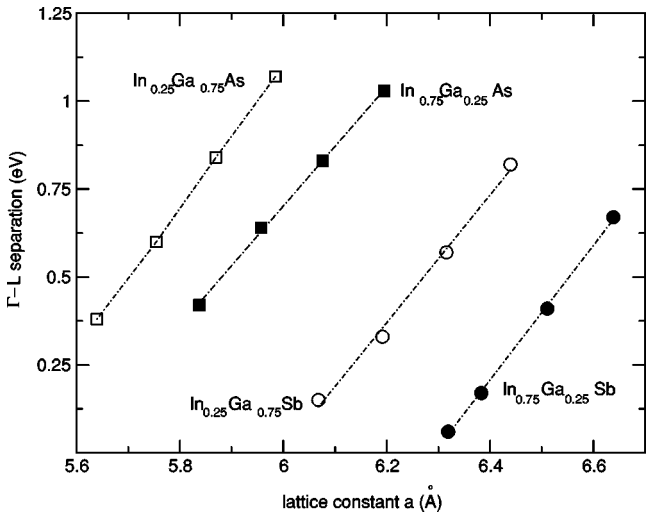

FIG. 3. SX-LDA $\overline{\Gamma}-\overline{L}$ separation (in eV) for the luzonite structures as a function of the cubic lattice constant (in Å): Ga-rich InGaAs (empty squares); In-rich InGaAs (filled squares); Ga-rich InGaSb (empty circles); In-rich InGaSb (filled circles).

leads to a widening of the band gap (the centers of the bands move apart). At the same time, both the valence band and the conduction band are broadened due to increasing overlap of the wave functions. This second effect tends to close the band gap and to drive the system towards a metallic state. As it turns out, the splitting of the bonding-antibonding states prevails and one observes a band gap widening with decreasing lattice parameter. Moreover, the distance dependence for both the direct gap as well as the indirect gap is fairly independent of the specific chemical nature of the cation in the III-V semiconductors investigated in this study. Furthermore, the $\overline{\Gamma}-\overline{L}$ separation is determined by an energy difference within a band and therefore depends primarily on the width of the conduction band, i.e., on the overlap of the states forming the conduction band. Since cationic *s* and *p* states dominate the conduction band, the width of the conduction band is related to the nature and distance of the cations. At distances characteristic for Ga-Ga and Ga-In equilibrium spacings in III-V semiconductors, the Ga and In wave functions are quite similar and size effects prevail over chemical effects.

The linear behavior of the direct band gap as a function of volume is a well-known and established result.[32] A linear relationships between band-gap and lattice parameter can be also obtained within a simple reduced-basis (i.e., cation *s* and anion *p* states) tight-binding model, assuming a Harrison-like[17] ($\sim 1/d^n$ where $n=2,3,4$ for $s-s, s-p$, and $p-p$ interactions, respectively) scaling law for the dependence of the first and second nearest-neighbor matrix elements on the atomic distance. Within this same picture, it is also reasonable to expect that the linear behavior is not strongly affected by chemical composition, given that the wave functions involved are very similar for In-Ga and As-Sb. On the other hand, due to the hybridized character of the lowest conduction states at $\overline{L}$ (mainly cation and anion *s* states), the linear behavior of the $\overline{\Gamma}-\overline{L}$ transition versus volume cannot be straightforwardly reproduced within such a simple model.

C. Composition dependence of direct and indirect band gaps

Let us first focus on the effect of anion substitution and compare the transitions considered in Ga-rich systems at the equilibrium lattice constant; we have $E^{\overline{\Gamma}-\overline{\Gamma}}_{Ga_{0.75}In_{0.25}As}=0.81$ eV, $E^{\overline{\Gamma}-\overline{L}}_{Ga_{0.75}In_{0.25}As}=1.41$ eV, $E^{\overline{\Gamma}-\overline{\Gamma}}_{Ga_{0.75}In_{0.25}Sb}=0.22$ eV and $E^{\overline{\Gamma}-\overline{L}}_{Ga_{0.75}In_{0.25}Sb}=0.54$ eV. Note that both the $\overline{\Gamma}-\overline{\Gamma}$ and $\overline{\Gamma}-\overline{L}$ energy transitions in InGaSb structures are much smaller than in InGaAs systems; moreover, we observe at a given cation composition, that the $\overline{\Gamma}-\overline{L}$ separation is $\Delta E^{\overline{\Gamma}-\overline{L}}_{In_xGa_{1-x}As}=0.60$ eV and $\Delta E^{\overline{\Gamma}-\overline{L}}_{In_xGa_{1-x}Sb}=0.32$ eV for As and Sb based systems, respectively. Therefore the As compounds seem to be more promising for TPV applications, due to a higher $\Delta E^{\overline{\Gamma}-\overline{L}}$ barrier.

Let us now investigate the composition dependence of these transitions in ternary systems. A complete study would of course imply the examination of disordered alloys: however, we can study the trend as a function of composition in ordered structures, considering only five different compositions: $x=0$ and 1 (binary compounds), $x=0.25$, 0.75 (luzonite structures), and $x=0.5$ (CuAu system). We decided to include the CuAu structure in our set since it can be considered equivalent to luzonite from the ordering point of view, both these systems are ordered structures having (001) as ordering vector.[10]

All the systems considered are particularly important in the context of disordered alloys, since, due to local atomic coordination, the ''local clusters'' they exhibit (i.e., In_3Ga, In_2Ga_2, and $InGa_3$ in In-rich luzonite, CuAu, and Ga-rich luzonite, respectively) can be regarded as building blocks of the disordered alloy. In order to be compared with cubic luzonite systems, the CuAu structure was also considered within cubic lattice constants, i.e., we neglected any tetragonal distortion of the cation sublattice.

In Table III, we show the experimental values[17,33] for the direct $\overline{\Gamma}-\overline{\Gamma}$ transitions in InGaAs alloys at different concentrations. Moreover, we report the SX-LDA values for the direct and indirect band gaps and for the $\overline{\Gamma}-\overline{L}$ separation in As-based systems and the character of the first conduction band at $\overline{\Gamma}$ and $\overline{L}$. Note that Cheng *et al.*[34] found a $\overline{\Gamma}-\overline{L}$ separation in $In_{0.53}Ga_{0.47}As$ of 0.55 eV from ultraviolet photoemission measurements, which is in very good agreement with the predicted SX-LDA value of 0.62 eV for Cu-Au $In_{0.5}Ga_{0.5}As$ system (see Table III). Upon alloying GaAs with In, the experimental energy band gap diminishes from 1.52 eV (pure GaAs) to 0.42 eV (pure InAs) while the lattice parameter expands from 5.653 Å for GaAs to 6.058 Å for InAs. This trend is reproduced by the self-consistent SX-FLAPW calculations including spin-orbit splitting. There is a pronounced deviation between the calculated and measured energy band gap for binary GaAs and for the composition $In_{0.25}Ga_{0.75}As$. Recall that the SX approach produces an error of about 0.3 eV for pure GaAs, so that this approach may strongly affect the final results for the Ga-rich ternary compounds. Moreover, it is likely that the actual arrangement of atoms in the experimental samples is different from the luzonite structure assumed in the calculations.

TABLE III. Experimental direct band gap and SX-LDA values for the direct, indirect transitions, and $\overline{\Gamma}-\overline{L}$ separation in InGaAs systems (all values are in eV—spin-orbit correction included). The character of the first conduction band at $\overline{\Gamma}$ and $\overline{L}$ is also shown. The experimental values refer to optical band gaps at 100 K in disordered alloys at the specified composition.

System	Expt $\overline{\Gamma}-\overline{\Gamma}$ gap	SX-LDA $\overline{\Gamma}-\overline{\Gamma}$ gap	SX-LDA $\overline{\Gamma}-\overline{L}$ gap	SX-LDA $\overline{\Gamma}-\overline{L}$ separ.	Character of cond. band at $\overline{\Gamma}$[d]	Character of cond. band at $\overline{L}$[d]
GaAs zinc-blende	1.52[a]	1.20	1.66	0.46	39% Ga-*s* 35% As-*s*	26% Ga-*s* 15% As-*s*
$In_{0.25}Ga_{0.75}As$ luzonite	~1.1[b]	0.81	1.41	0.60	30% Ga-*s* 5% In-*s* 32% As-*s*	0% Ga-*s* 8% In-*s* 16% As-*s*
$In_{0.5}Ga_{0.5}As$ CuAu	~0.8[b]	0.62	1.25	0.63	22% Ga-*s* 17% In-*s* 28% As-*s*	23% Ga-*s* 7% In-*s* 12% As-*s*
$In_{0.75}Ga_{0.25}As$ luzonite	~0.6[b]	0.48	1.11	0.63	11% Ga-*s* 25% In-*s* 33% As-*s*	23% Ga-*s* 0% In-*s* 13% As-*s*
InAs zinc-blende	0.42[c]	0.44	1.63	1.19	34% In-*s* 31% As-*s*	26% In-*s* 13% As-*s*

[a]See Ref. 16, and references therein.
[b]Reference 33.
[c]Reference 17.
[d]The charge of a band state is normalized to 100% in the unit cell. If a cell contains, for example, three equivalent Ga atoms, then the value shown is the contribution per Ga atom multiplied by 3. It should be noted, however, that the specific value depends on the size of the muffin-tin radius used in the expansion of the wave functions.

Let us now discuss the angular character of the most relevant states. The orbital character of the states at the top of the valence band at $\overline{\Gamma}$ is predominantly As-*p*. The wave function at the bottom of the conduction band has cationic *s* character. Due to the more delocalized nature of the In 5*s* wave functions compared with the Ga 4*s* functions, there is more Ga-*s*-like charge in GaAs (39% of the wave function is localized within the Ga sphere) compared with the In-*s*-like charge in InAs (34% in the In sphere), as can be seen from Table III. It should be kept in mind, however, that the absolute value of an *l*-like charge depends on the choice of the muffin-tin radius used in the basis set expansion. The intermediate stoichiometries show a rather smooth variation of the *s*-like charge inside the Ga and In spheres ($R_{MT}^{Ga}=2.25$ a.u. and $R_{MT}^{In}=2.62$ a.u.).

The situation at the $\overline{L}$ point is different due to symmetry effects. If one assumes that near the $A_{0.25}B_{0.75}C$ composition the dominant atomic arrangement of the alloy can be described by the luzonite structure, then the conduction-band minimum at $\overline{L}$ has the *s* character of the cation *B*, but no *s* character of the *A*-type atoms. In other words, even for an In-rich alloy of the form $In_{0.75}Ga_{0.25}As$, the conduction-band minimum at $\overline{L}$ has Ga-*s* character, hybridized with As-*s* states. In the limiting case of vanishing Ga content, i.e., for pure InAs, one finds, of course, that the conduction-band minimum at $\overline{L}$ has In *s* character, hybridized with As-*s* states. As a consequence, one notes a fairly nonlinear behavior of the $\overline{\Gamma}-\overline{L}$ separation in the series between GaAs and InAs. For pure GaAs, the computed $\Gamma-L$ separation is about 0.5 eV; this value remains almost constant (around 0.6 eV) up to about 75% In and then rises steeply to the value of 1.19 eV for pure InAs.

In Fig. 4(a), the SX-LDA values for the direct transitions in InGaAs (circles) and InGaSb (stars), respectively, are shown together with a parabolic fit. The trend of the direct band gap versus composition is well represented by a parabolic behavior: $E^{\overline{\Gamma}-\overline{\Gamma}}_{In_{1-x}Ga_xSb}=(x)E^{\Gamma-\Gamma}_{GaSb}+(1-x)E^{\Gamma-\Gamma}_{InSb}+b^{\overline{\Gamma}-\overline{\Gamma}}_{In_xGa_{1-x}Sb}x(1-x)$, where $b^{\overline{\Gamma}-\overline{\Gamma}}_{In_xGa_{1-x}Sb}$ is commonly denoted as the ''bowing coefficient.'' In our case, $b^{\overline{\Gamma}-\overline{\Gamma}}_{In_xGa_{1-x}Sb}=1.12$ eV and $b^{\overline{\Gamma}-\overline{\Gamma}}_{In_xGa_{1-x}As}=0.89$ eV, so that both As- and Sb-based compounds show an appreciable deviation from linearity, mainly due to ordering effects. Moreover, the energy range that the direct gap can span is larger in As-based ($\Delta_{InGaAs}=0.78$ eV) than in Sb-based ($\Delta_{InGaSb}=0.21$ eV) compounds; therefore InGaAs systems appear to be more suitable for band-gap tuning purposes.

We show in Fig. 4(b) the composition dependence of SX-LDA energy values for the first and second conduction-band

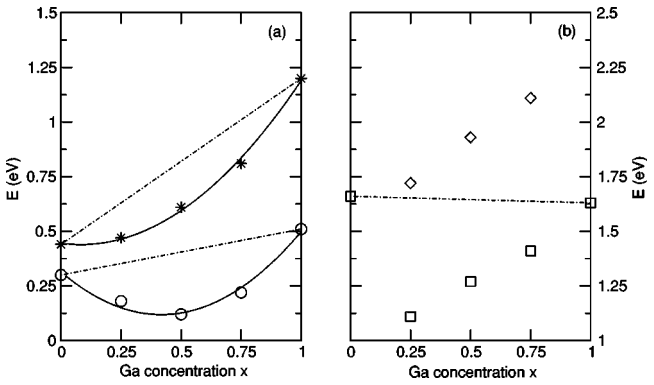

FIG. 4. (a) SX-LDA direct band gaps (in eV) for InGaAs (circles) and InGaSb (stars) systems versus Ga concentration (the dot-dashed line shows a linear average of the direct band gaps in the binaries). (b) SX-LDA lowest (squares) and second-lowest (diamonds) indirect band gaps at $\overline{L}$ in InGaAs systems (the dot-dashed line shows a linear average of the indirect band gap in the binaries).

states at $\overline{L}$ (with respect to the valence-band maximum) in InGaAs systems (the situation is absolutely equivalent in Sb-based structures). Here the repulsion (i.e., the difference between the two energy values shown at a given composition x) due to the superlattice perturbative potential is rather large (about half an eV) for all the structures. Furthermore, let us consider again the angular character and degeneracy of the different conduction states we find: in In-rich luzonites ($x=0.25$), the lowest state at $\overline{L}$ is a singly degenerate state with Ga-s character whereas the second lowest state is three-fold degenerate with In-s character; on the other hand, in Ga-rich luzonite ($x=0.75$), the situation is reversed, with the lowest level being a three-fold degenerate state localized on the Ga sublattice and the upper single degenerate state being localized on the In sublattice. Now, the singly degenerate state shows a large shift with respect to the linear average of the binary levels [dot-dashed line in Fig. 4(b)], whereas this same shift is lower for the three-fold state. As a result, the strongest reduction in the $\overline{\Gamma}-\overline{L}$ transition is obtained for In-rich systems, which seems therefore to be the more promising for thermovoltaic and, possibly, other applications. Moreover, as a last remark, note that in the CuAu structures these two states are both singly degenerate and localized on the Ga site (lowest level) and on the In site (upper level); in this case, the shift with respect to the linear average is more or less equivalent for the two superlattice states.

IV. CONCLUSIONS

Screened-exchange LDA calculations were performed for simple ordered ternary InGaAs and InGaSb systems, in order to investigate the dependence of the direct and lowest indirect band gap as a function of pressure and composition. Our results can be summarized as follows: (i) both the direct and indirect band $\overline{\Gamma}-\overline{\Gamma}$ and indirect $\overline{\Gamma}-L$ band gap decrease linearly as the lattice parameter is increased; (ii) the reduction is two times faster for the direct than for the indirect band gap; (iii) the slope of this linear behavior is nearly independent of the chemical composition; (iv) the direct band gap shows a parabolic dependence on the ternary concentration with a non-negligible bowing parameter (i.e., about 1 eV). Therefore pressure as well as composition can be used as valid tools to vary the transitions considered; in particular, due to the symmetry properties of the ternary luzonites, In-rich systems show a strong reduction of the $\overline{\Gamma}-\overline{L}$ transition, compared to the linear average of the $\Gamma-L$ band gaps in binaries. Finally, As-based systems are predicted to have larger $\overline{\Gamma}-\overline{L}$ gaps than Sb-based luzonites and therefore seem to be more promising for achieving high carrier mobilities in TPV device applications.

ACKNOWLEDGMENTS

Work at Northwestern University was supported by the National Science Foundation (through the Northwestern University Materials Research Center). Grants of computer time at the CINECA supercomputing center (Bologna, Italy) through the Istituto Nazionale di Fisica della Materia (INFM) are aslo acknowledged.

*Permanent address: Toyota Central R&D Laboratories, Inc., Nagakute, Aichi 480-1192, Japan.

[1] K. Shim and H. Rabitz, Phys. Rev. B **57**, 12 874 (1998).
[2] See J.C. Woicik, J. G. Pellegrino, B. Steiner, K. E. Miyano, S. G. Bowpadre. L. B. Soreusen, T.-L. Lee, and S. Khalid, Phys. Rev. Lett. **79**, 5026 (1997); F. Boscherini, C. Lamberti, S. Pascarelli, C. Rigo, and S. Mobilio, Phys. Rev. B **58**, 10 745 (1998), just to name a few recent experimental studies.
[3] See L. Bellaiche and A. Zunger, Phys. Rev. B **57**, 4425 (1998); L.-W. Wang and A. Zunger, *ibid.* **56**, 12 395 (1997); L.-W. Wang, L. Bellaiche, S.-H. Wei, and A. Zunger, Phys. Rev. Lett. **80**, 4725 (1998); A. Zunger, MRS Bull. **22**, 20 (1997), just to name some recent papers.
[4] S.H. Wei, L.G. Ferreira, J.E. Bernard, and A. Zunger, Phys. Rev. B **42**, 9622 (1990).
[5] K.A. Mader and A. Zunger, Phys. Rev. B **51**, 10 462 (1995).
[6] S.-H. Wei and A. Zunger, Phys. Rev. B **57**, 8983 (1998).
[7] H.W.M. Salemink and O. Albrektsen, Phys. Rev. B **47**, 16 044 (1993); S. Perkowitz, L.S. Kim, and P. Becla, *ibid.* **43**, 6598 (1991).
[8] D.B. Zax, D. Zamir, and S. Vega, Phys. Rev. B **47**, 6304 (1993).
[9] L. Subramanian and W. Wolf (private communications).
[10] S.-H. Wei and A. Zunger, Phys. Rev. B **39**, 3279 (1989).
[11] P. Hohenberg and W. Kohn, Phys. Rev. **136**, B864 (1964); W. Kohn and L.J. Sham, Phys. Rev. **145**, 561 (1966).
[12] E. Wimmer H. Krakauer M. Weinert, and A.J. Freeman, Phys. Rev. B **24**, 864 (1981); H.J.F. Jansen and A.J. Freeman, *ibid.* **30**, 561 (1984).
[13] D.M. Bylander and L. Kleinman, Phys. Rev. B **41**, 7868 (1990).
[14] A. Seidl, A. Görling, P. Vogl, J.A. Majewski, and M. Levy, Phys. Rev. B **53**, 3764 (1996).
[15] W. Wolf, E. Wimmer, S. Massidda, M. Posternak, and C.B. Geller, Bull. Am. Phys. Soc. **43**, 797 (1998).
[16] R. Asahi, W. Mannstadt, and A.J. Freeman, Phys. Rev. B **59**, 7486 (1999).
[17] See, for example, W. Harrison, *Electronic Structure and the Properties of Solids* (Freeman, San Francisco, 1980).
[18] L. Hedin and B.I. Lundqvist, J. Phys. C **4**, 2064 (1971).
[19] H.J. Monkhorst and J.D. Pack, Phys. Rev. B **13**, 5188 (1976).

[20] S. Massidda, A. Continenza, A.J. Freeman, T.M. de Pascale, F. Meloni, and M. Serra, Phys. Rev. B **41**, 12 079 (1990).
[21] D.S. Wang, R. Wu, and A.J. Freeman, Phys. Rev. B **47**, 14 932 (1993).
[22] *Numerical Data and Functional Relationships in Science and Technology*, Landolt-Bornstein, Group III, Vol. 17, Pt. a (Springer-Verlag, Berlin, 1982).
[23] We recall that previous calculations (see, for example, Ref. 27) have shown that predictions according to Vegard's rule are in good agreement (within 1%) with those obtained from total energy minimizations and from experimental data.
[24] Note that clear illustrations and structural details of the luzonite structure can be found in Ref. 10.
[25] T.H. Glisson, J.R. Hauser, M.A. Littlejohn, and C.K. Williams, J. Electron. Mater. **7**, 1 (1978).
[26] S.-H. Wei and A. Zunger, Appl. Phys. Lett. **58**, 2684 (1991).
[27] S. Picozzi, A. Continenza, and A.J. Freeman, Phys. Rev. B **52**, 5247 (1995).
[28] S.-H. Wei and A. Zunger, J. Appl. Phys. **63**, 5794 (1988).
[29] The calculated value for the spin-orbit coupling for the In-rich InGaSb luzonite was $\Delta_{so} \sim 0.75$ eV.
[30] Recall that since the volume is related to pressure through the nonlinear Murnaghan equation of state [F.D. Murnaghan, Proc. Natl. Acad. Sci. USA **30**, 244 (1944)], the band gaps show a quadratic behavior as a function of pressure (see, for example, Ref. 32).
[31] C.S. Menoni, H.D. Hochheimer, and I.L. Spain, Phys. Rev. B **33**, 5896 (1986); A.R. Goni, K. Strossner, K. Syassen, and M. Cardona, *ibid.* **36**, 1581 (1987); S. Ves, K. Strössner, Chul Koo Kim, and M. Cardona, Solid State Commun. **55**, 327 (1985).
[32] S. Ves, U. Schwarz, N.E. Christensen, K. Syassen, and M. Cardona, Phys. Rev. B **42**, 9113 (1990).
[33] A.E. Taylor and E. Fortin, Can. J. Phys. **48**, 1874 (1970).
[34] K.Y. Cheng, A.Y. Cho, S.B. Christman, T.P. Pearsall, and J.E. Rowe, Appl. Phys. Lett. **40**, 423 (1982).